Nuclear Inst. and Methods in Physics Research, A 960 (2020) 163662

Contents lists available at ScienceDirect

Nuclear Inst. and Methods in Physics Research, A

journal homepage: www.elsevier.com/locate/nima

A new SiPM-based positron annihilation lifetime spectrometer using LYSO and LFS-3 scintillators

H.B. Wang, Q.H. Zhao, H. Liang *, B.C. Gu, J.D. Liu, H.J. Zhang, B.J. Ye *

State Key Laboratory of Particle Detection and Electronics, University of Science and Technology of China, Hefei 230026, China

ARTICLE INFO

Keywords:
Positron annihilation lifetime spectrometer
Time resolution
SiPM
LYSO
LFS-3

ABSTRACT

Positron annihilation lifetime (PAL) spectroscopy is a unique technique to characterize atomic-scaled microstructure of materials, especially the vacancy-type defects. Compared to photomultiplier tube, silicon photomultiplier (SiPM) has a higher quantum efficiency, a more compact size, and a much lower price. Considering the evident advantages of SiPM, we developed a SiPM-based PAL (SiPM-PAL) spectrometer by using LFS-3 and LYSO scintillators in the sizes of $3\times3\times l$ mm^3. The performance of the SiPM-PAL spectrometer was studied with four different scintillator lengths (l) of 5.0, 9.5, 13.8, and 20.0 mm. Under the same experimental conditions, with LFS-3 scintillator length decreasing from 20.0 to 5.0 mm, the time resolution (in FWHM) of SiPM-PAL spectrometer was significantly improved from 174.9 to 135.9 ps. While for the SiPM-PAL spectrometer with LYSO scintillators, the time resolution improved from 181.9 to 137.0 ps with scintillator length decreasing from 20.0 to 5.0 mm. Compared to conventional PAL spectrometer using photomultiplier tubes, a novel, small size, and low cost PAL spectrometer is successfully constructed by using SiPMs. Easy customization and superiority in time resolution and small size of SiPM-based scintillation detectors guarantee high flexibility and adaptability to the SiPM-PAL spectrometers, positron micro-beam facilities, and angular correlation of positron annihilation radiation measurements.

1. Introduction

Positron annihilation lifetime (PAL) technique has been well known as a useful method to study defects in condensed matters [1–3]. To improve the performance of PAL spectrometer, lots of efforts have been made to improve its time resolution and count rate [4–7]. A typical PAL spectrometer uses a configuration of two detectors (each detector constructed by using a BaF_2 scintillator and a photomultiplier tube (PMT)), two constant fraction differential discriminators, a time-to-amplitude converter, and a multichannel analyzer [8].

Several new configurations of digital oscilloscope or fast commercial digitizer were also applied in PAL spectrometer [9–11]. Conventional PAL spectrometers utilize scintillators and PMTs. With rapid development of silicon photomultiplier (SiPM) technique, more and more researchers attempt to use SiPMs to construct scintillation detectors to detect γ rays. Compared to PMT, SiPM exhibits numerous advantages including higher quantum efficiency, higher single photon time resolution, more compact size, lower power consumption, much lower price, and insensitivity to magnetic field [12].

Due to high detection efficiency and capability to detect a single photon, SiPMs are demonstrated to be suitable for excellent timing performance [13]. In the past few years, SiPMs have been widely applied to particle physics experiments, medical facilities, and automotive light detection and ranging (LiDAR) systems, due to the fast timing characteristics [14–16]. Inspired by the fast development of SiPM technique, SiPM is naturally considered as a promising photodetector to further improve the time resolution of PAL spectrometer.

Recent years, LYSO ($Ce_x(Lu, Y)_{1-x}SiO_5$) and LFS-3 (lutetium fine silicate) scintillators which exhibit excellent time resolution and energy resolution, are increasingly used to construct detectors for TOF-PET (time-of-flight positron emission tomography) scanners [17,18]. The performances of LYSO and LFS-3 scintillators can provide high stopping power, fast decay time, high throughput, high light yield, and are non-hygroscopic [19]. In consequence, LYSO and LFS-3 scintillators are considered as promising scintillators to further improve the time resolution and count rate of PAL spectrometers.

Time resolution and count rate are usually considered as the most critical parameters of PAL spectrometer. The length of scintillator is the key to balance time resolution and count rate of a PAL spectrometer. Thereafter, in the present work, we coupled LYSO and LFS-3 crystals with different lengths to SiPMs to reveal the effect of scintillator length on the performance of SiPM-based PAL spectrometer.

* Corresponding authors.
E-mail addresses: simonlh@ustc.edu.cn (H. Liang), bjye@ustc.edu.cn (B.J. Ye).

https://doi.org/10.1016/j.nima.2020.163662
Received 6 June 2019; Received in revised form 15 February 2020; Accepted 15 February 2020
Available online 17 February 2020
0168-9002/

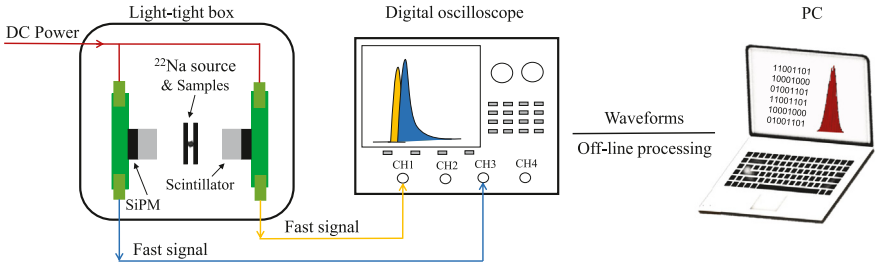

Fig. 1. Schematic of CRT measurement setup.

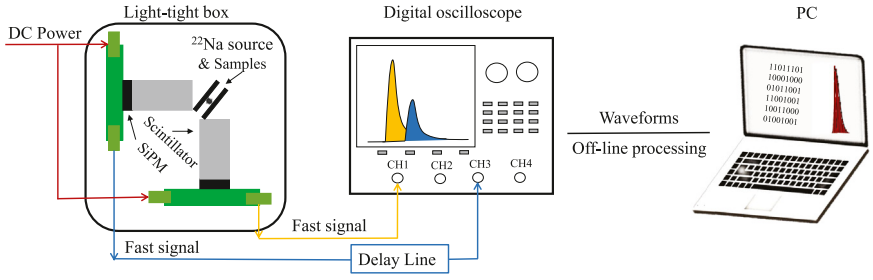

Fig. 2. Schematic of PAL measurement setup.

Table 1
The principal properties of LYSO and LFS-3 scintillators.

	LYSO	LFS-3
Density (g/cm^3)	7.1	7.35
Attenuation length for 511 keV (cm)	1.2	1.15
Decay time (ns)	36	33–36
Luminescence (nm) at peak	420	425
Light yield (×10^3 photons/MeV)	33	37–38
Refractive index	1.81	1.81
Hygroscopic	No	No

2. Experimental technique and analysis methods

2.1. Experimental technique

LYSO scintillator (Saint-Gobain, France) is a cerium-doped lutetium based scintillation crystal. LFS-3 (Zecotek Photonics Inc., Canada) is a set of Ce-doped silicate scintillators comprising of lutetium and crystallized in the monoclinic system. The principal properties of LYSO and LFS-3 scintillators that obtained from the manufacturers, are listed in Table 1. With a peak wavelength emission of around 420 nm, the outputs of these two scintillators are suitable for the sensitivity curve of SiPMs [12,17].

The scintillators were cut and polished into the sizes of $3 \times 3 \times l$ mm^3 with four different lengths (l) of 5.0, 9.5, 13.8, and 20.0 mm. The scintillators were fully wrapped by polytetrafluoroethylene (Teflon) films, except the narrow region (3×3 mm^2) connected to SiPM. The Teflon-wrapped scintillator was coupled to SiPM by using silicone optical grease (DC200, Dow Corning Corp.).

The SiPMs (MicroFJ 30035, SensL) are in a dimension of 3.07×3.07 mm^2 sensor active area which provided good light collection and well matched cross section of the LYSO and LFS-3 scintillators. The SiPMs were mounted on evaluation boards which have fast signal outputs. SiPMs which produced by SensL have ultra-fast output signal that is capacitively modified for the standard silicon photomultiplier structure to address the challenges of low light signal sensing, timing and quantization to single photon levels.

A ^{22}Na positron source (activity of around 1.85 MBq) was encapsulated between two identical Kapton foils ($17 \times 10 \times 0.0075$ mm^3). The positron source was sandwiched between two identical GaN samples ($10 \times 10.5 \times 0.35$ mm^3).

Both coincidence resolving time (CRT) and PAL measurements were performed in this work. The CRT method measured the time difference between the time stamps of two simultaneous annihilation photons (511 keV). Positron annihilation lifetime spectra comprise measurements of the time delay between the birth signal of a positron (1275 keV photon) and annihilation signal (511 keV photon). All measurements were performed in 3D-printed light-tight box which is wrapped in a blackout cloth to ensure a dark environment. The detector signals were directly connected to the digital oscilloscope via SMA-to-BNC coaxial cables. All measurements were performed at room temperature (around 25 °C) by using a high accuracy DC power supply (IT6953A, ITECH Electronic Corp.). The operating bias of SiPM was increased from 30 to 34 V in steps of 0.5 V. The output signals of detectors were recorded by the digital oscilloscope.

To evaluate the performance of scintillation detectors for PAL spectrometer, a CRT measurement setup was implemented using a fast digital oscilloscope (H8404, LeCroy Corp.) with a bandwidth of 2 GHz and a sampling rate of 20 GS/s. The output signals from the two detectors were recorded with 9-bit signal storage accuracy. The measurements were performed with two SiPM-based scintillation detectors (LYSO or LFS-3 coupled to a SiPM for each detector) in a back-to-back configuration within a light-tight box. The schematic of the CRT measurement is shown in Fig. 1.

To carry out positron annihilation lifetime experiments, a SiPM-based PAL measurement setup was constructed. As shown in Fig. 2, the setup comprises two scintillation detectors (LYSO or LFS-3 coupled to a SiPM for each detector) which were positioned in a triangular geometry configuration. The stop detector signal was delayed for around 5 ns through a coaxial cable.

2.2. Analysis methods

The fast signals of two detectors were digitized and stored by using the digital oscilloscope for both CRT and PAL measurements. Different oscilloscope settings (acquisition time windows and triggers) were utilized for CRT and PAL measurements. The time resolutions of the two setups were determined under different time thresholds and bias voltage conditions. The PAL measurements were performed using the optimal detector timing resolution settings (SiPM bias voltage and discrimination threshold), which were derived from the CRT measurements.

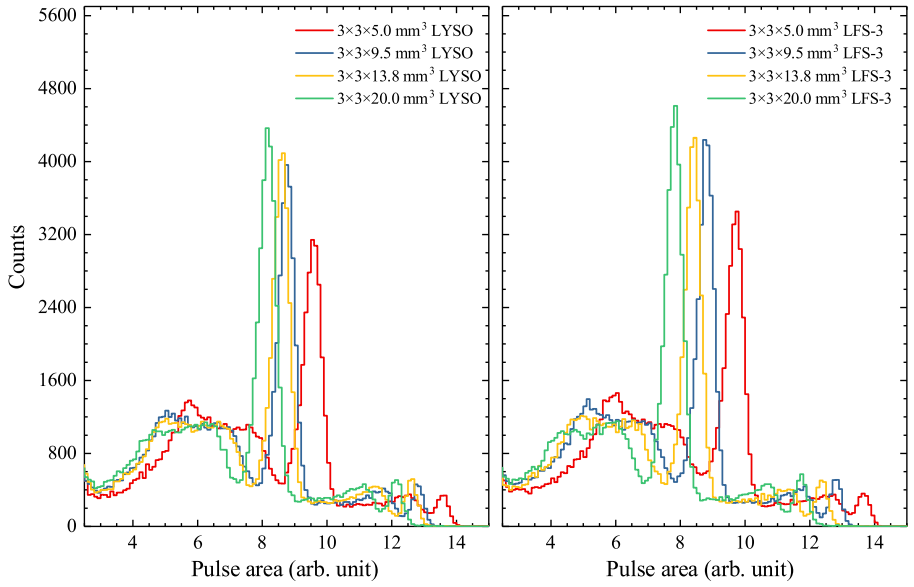

Fig. 3. Energy spectra recorded by LYSO and LFS-3 scintillators length of 5.0, 9.5, 13.8, and 20.0 mm at a SiPM bias voltage of 33.5 V.

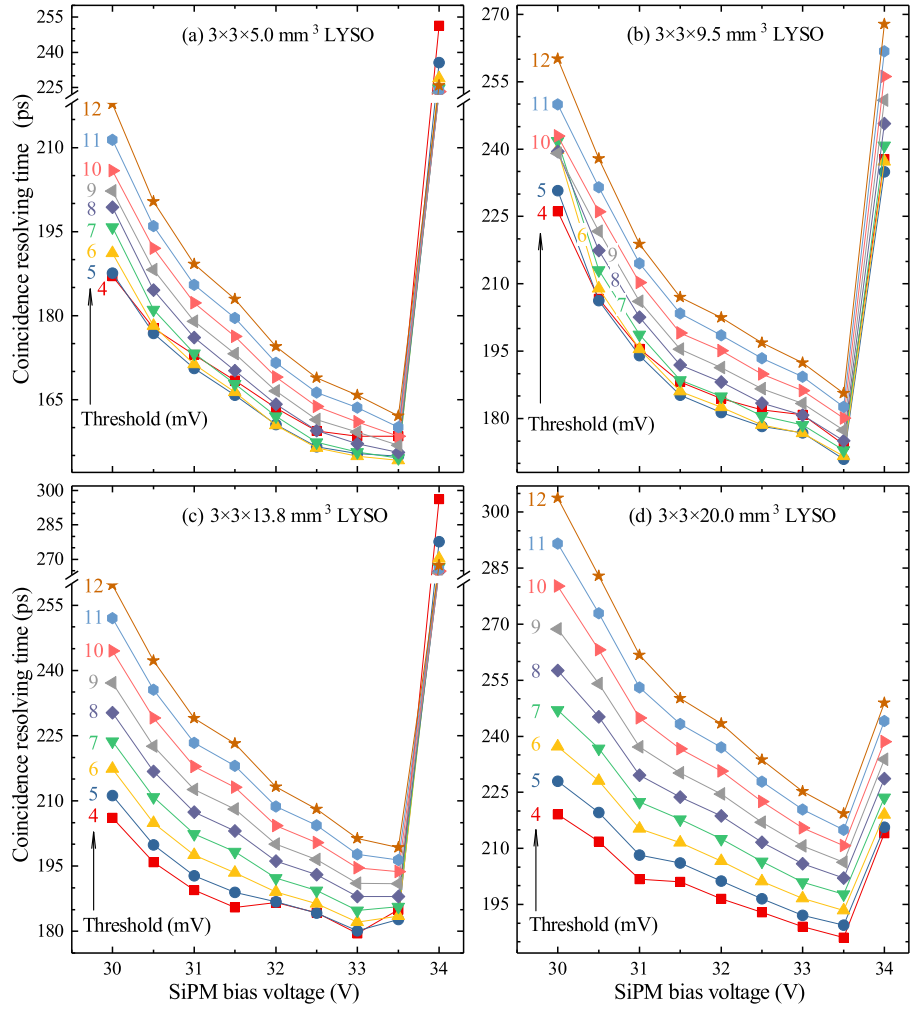

Fig. 4. Variations of CRT as a function of SiPM bias voltage for LYSO scintillator length of (a) 5.0 mm, (b) 9.5 mm, (c) 13.8 mm, and (d) 20.0 mm. The colorful numbers denote LED thresholds.

For each event, in both measurement setups, the photon arrival time at each detector was determined from the rising part of waveform by applying a leading-edge discrimination (LED) time pick-off method. The energy deposition in scintillators due to the 511 keV annihilation

photon and 1275 keV prompt photon were measured by integrating the fast signals area.

A polynomial fitting function was used to fit the rising part of digitized signals between baseline and 40% of pulse maximum and so enable the extraction of a time-stamp by applying an appropriate LED method. For CRT measurements, the events were recorded by setting an energy window within the full width at tenth maximum (FWTM) of the 511 keV total absorption peak. For the start signals of PAL measurements, pulses were accepted with pulse area corresponding to photon energies from the 1275 keV Compton edge up to and including the entire 1275 keV total absorption peak. While for the stop signals of the PAL measurements, all events within the FWTM of 511 keV total absorption peak were recorded. To find the thresholds yielding the optimal CRT, the LED thresholds were swept from the earliest portions of the rising edge of signals. To find the bias voltage that providing the best timing performance for CRT measurements, the signals were processed with a bias voltage increasing from 30.0 to 34.0 V in steps of 0.5 V.

3. Results and discussion

3.1. Energy spectra

To analyze the time resolution of SiPM-PAL spectrometer, it is a vital task to make events selection using energy cut for CRT and PAL measurements. Energy spectra of γ rays were obtained by integrating the fast signal area for LYSO and LFS-3 scintillators with four different lengths of 5.0, 9.5, 13.8, and 20.0 mm at a SiPM bias voltage of 33.5 V. The energy distribution, which corresponds to the number of counts as a function of pulse area, is presented in Fig. 3. The 511, 1275 keV total absorption peaks, and Compton edge of 1275 keV total absorption peak are clearly to be distinguished. For CRT measurement, the energy windows were set within the FWTM of the 511 keV total absorption peak. As for PAL measurement, the energy window was set within an energy range from the 1275 keV Compton edge up to the entire 1275 keV total absorption peak and the FWTM of 511 keV total absorption peak.

3.2. CRT vs. SiPM bias voltage, LED threshold, and scintillator length

Coincidence resolving time (CRT) measurements were conducted at bias voltages from 30.0 to 34.0 V in steps of 0.5 V. The bias voltage sweep curves were obtained for LYSO and LFS-3 scintillators with four different lengths of 5.0, 9.5, 13.8, and 20.0 mm. The CRT values were derived from Gaussian fitting of histogram of time difference between the two 511 keV photons from the same annihilation event. More than 20,000 events were selected (within the full width at tenth maximum of the 511 keV total absorption peak) for the Gaussian fitting for a single histogram.

It is well known that, CRT depends on both SiPM bias voltage and discrimination threshold. The variations of CRT as a function of SiPM bias voltage and LED threshold of LYSO are shown in Fig. 4. It is clear that, for the same scintillator length and LED threshold, the CRT value initially drops drastically with SiPM bias voltage increasing from 30.0 to 33.5 V, and then abruptly increases at the bias voltage of 34.0 V. At the high reverse bias voltage of 34.0 V, the dark current of SiPM has a very steep increase due to the reverse breakdown of the SiPM microcell. The minimum CRT of each scintillator length is achieved at the bias voltage of around 33.5 V. Additionally, for the same LYSO scintillator length and bias voltage, the CRT value is gradually optimized with the LED threshold decreasing from 12 to 4 mV. The CRT values at the LED threshold range between 4 and 6 mV are much better than those at higher LED thresholds.

To show the influence of LYSO scintillator length on CRT, the minimum CRT values in the SiPM bias voltage range from 30.0 to 34.0 V and LED threshold range from 4 to 12 mV at four lengths which are extracted from Fig. 4, are plotted in Fig. 5. The corresponding SiPM bias voltage and LED threshold of each minimum CRT are listed in square brackets, respectively. Fig. 5 shows a monotonous positive correlation between LYSO scintillator length and minimum CRT. The increase in CRT at longer scintillator length is due to the degrading of both light transfer efficiency and light transfer time spread in the longer scintillator [20]. At the shortest LYSO scintillator length of 5.0 mm, a good CRT of 154.2 ps is successfully obtained.

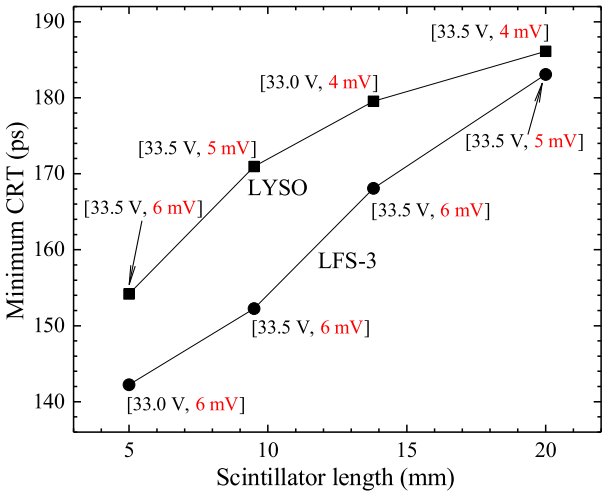

Fig. 5. Minimum CRT (SiPM bias voltages from 30.0 to 34.0 V, LED thresholds from 4 to 12 mV) as a function of scintillator length for LYSO (square symbols) and LFS-3 (circle symbols). The corresponding SiPM bias voltage and LED threshold of each minimum CRT are shown in black and red in square brackets, respectively.

For LFS-3 scintillators, CRT measurements were performed using the same experimental conditions (scintillator lengths, SiPM bias voltages, and LED thresholds) of LYSO. As shown in Fig. 6, the CRT results of LFS-3 are indicated in the same style of Fig. 4. Comparing the LYSO results with those from LFS-3 similar tends in CRT as a function of SiPM bias voltage and LED threshold were observed. The minimum CRT for each scintillator length is also obtained for a bias voltage of approximately 33.5 V. The minimum CRT values for the SiPM bias voltages of 30.0–34.0 V and LED thresholds of 4–12 mV at four lengths that extracted from Fig. 6, are also plotted in Fig. 5.

The minimum CRT degraded significantly with LFS-3 scintillator length increasing from 5.0 to 20.0 mm. The best CRT, 142.2 ps, was obtained using the shortest LFS-3 scintillator length of 5.0 mm, and is approximately 8% sorter than that from the LYSO scintillators of the same length. This is attribute to the faster decay time and higher light yield of LFS-3 as listed in Table 1. Overall, the aforementioned CRT results of scintillation detectors provide a clear guideline to improve the SiPM-PAL spectrometer time resolution.

3.3. Time resolution and count rate of SiPM-PAL spectrometer vs. scintillator length

To test the performance of SiPM-PAL spectrometer, PAL measurements were carried out at the SiPM bias voltage and LED threshold of each minimum CRT which were listed in the square brackets in Fig. 5. The PAL spectra of GaN were collected using LYSO and LFS-3 scintillators in four different lengths, as shown in Fig. 7. The total counts of 4×10^6 were collected for each spectrum.

The standard computer program LTv9, which is based on Gauss-Newton non-linear fitting routines, is utilized to analyze the spectra [21]. A PAL spectrum which consists of several decaying exponentials convoluted with the time resolution function of the PAL measurement system, could be written as a histogram $N(t)$ [22] in the form of:

$$N(t) = \sum_{j=1}^{k_0} [A_j \exp(-t/\tau_j)] \otimes R(t) + B \quad (1)$$

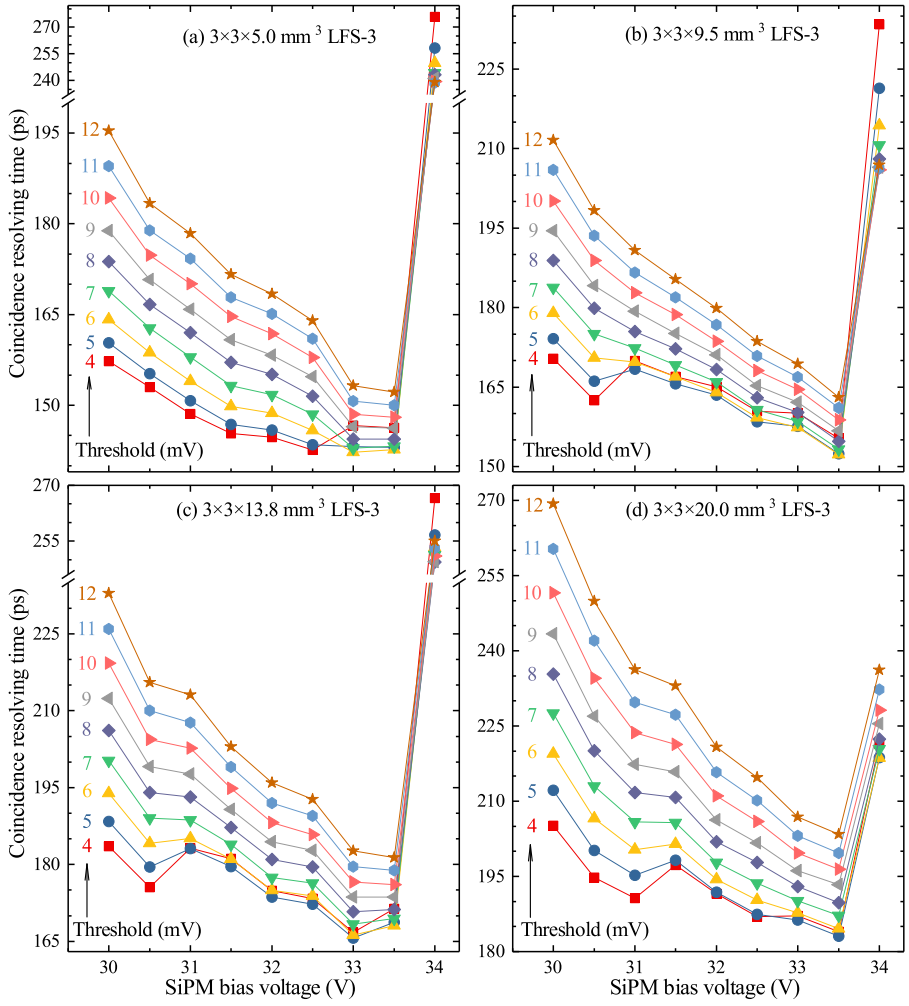

Fig. 6. Variations of CRT as a function of SiPM bias voltage for LFS-3 scintillator length of (a) 5.0 mm, (b) 9.5 mm, (c) 13.8 mm, and (d) 20.0 mm. The colorful numbers denote LED thresholds.

Table 2
Analysis results of PAL spectra of GaN which were measured by SiPM-PAL spectrometer with LYSO and LFS-3 scintillators.

	Length (mm)	τ_1 (ps)	τ_2 (ps)	I_1 (%)	I_2 (%)	Time resolution (ps, in FWHM)	count rate (cps)
LYSO	5.0	156.5 ± 0.2	398.1 ± 1.5	86.2 ± 0.1	13.8 ± 0.1	137.0	14.8 ± 1.4
	9.5	156.8 ± 0.3	399.1 ± 3.2	86.3 ± 0.2	13.7 ± 0.2	160.6	33.4 ± 2.3
	13.8	155.3 ± 0.3	390.6 ± 3.3	85.6 ± 0.2	14.4 ± 0.2	176.6	43.1 ± 2.4
	20.0	156.8 ± 0.4	401.7 ± 2.6	86.5 ± 0.2	13.5 ± 0.2	181.9	46.7 ± 4.0
LFS-3	5.0	155.6 ± 0.4	392.6 ± 4.1	85.7 ± 0.3	14.3 ± 0.3	135.9	15.8 ± 1.6
	9.5	155.2 ± 0.4	389.6 ± 3.3	85.6 ± 0.2	14.4 ± 0.2	148.9	38.9 ± 2.1
	13.8	154.6 ± 0.3	386.2 ± 1.1	85.1 ± 0.1	14.9 ± 0.1	166.4	44.0 ± 2.4
	20.0	157.0 ± 0.4	395.7 ± 1.7	86.2 ± 0.1	13.8 ± 0.1	174.9	45.2 ± 3.8

where t, k_0, R, B, τ_j, A_j are the time, number of lifetime components, time resolution function, background, mean lifetime of the jth lifetime component, and a pre-exponential factor ($A_j\tau_j$ is the "area" of the lifetime component), respectively. The time resolution function $R(t)$ [23] of a PAL system is usually written as:

$$R(t) = \frac{1}{\sigma\sqrt{2\pi}} \exp\left(-\frac{(t - T_0 - \Delta t)^2}{2\sigma^2}\right) \quad (2)$$

where T_0 represents the time-zero channel number (start channel), σ is the standard deviation, and Δt is a displacement. The objective of the analysis is to extract the lifetime components from the raw experimental spectra. Time resolution value is the FWHM ($2\sigma\sqrt{2\ln 2}$) of the timing resolution function. The time resolution in FWHM, two lifetime components, and their corresponding intensities which were resolved from all PAL spectra by using LTv9 program, are listed in Table 2.

As presented in Table 2, all PAL spectra of GaN measured by SiPM-PAL spectrometer with different scintillators (including scintillator material and length) give very close results including τ_1 (154.6–157.0 ps), τ_2 (386.2–401.7 ps), I_1 (85.1–86.5%), and I_2 (13.5–14.9%) values. This clearly indicates that, the SiPM-PAL spectrometer is successfully constructed by using LYSO and LFS-3 scintillators. The reliability of SiPM-PAL spectrometer is independent of scintillator length for both two scintillator materials of LYSO and LFS-3. The shorter lifetime component (τ_1) of around 156 ps is the positron lifetime in the defect-free bulk of the GaN. The longer lifetime component (τ_2) is from the positron annihilation in ^{22}Na source and the two source-sealing Kapton foils. The lifetime components (τ), intensities (I), and errors are local

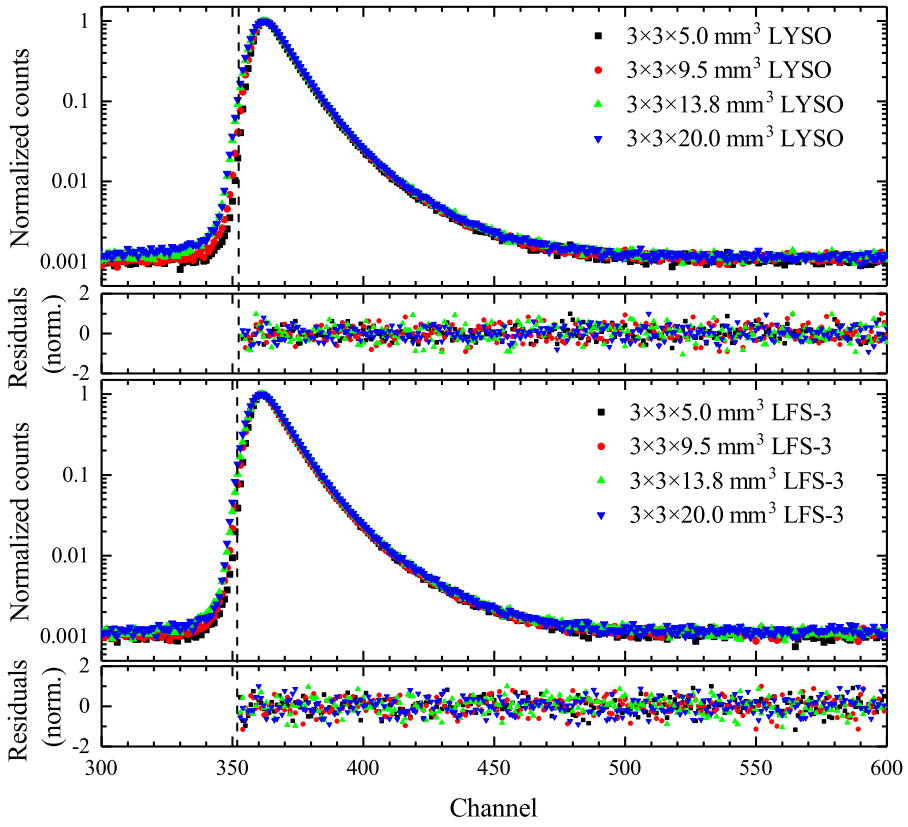

Fig. 7. PAL spectra of GaN which were measured by SiPM-PAL spectrometer with LYSO and LFS-3 scintillators. The right part of dash line (channel 354) in the spectra was used for PAL analysis. The channel width is 20 ps.

optimum values from the fitting process by using LTv9 program. A very small disturbance (such as random noise during the measurement) in the experimental data may induce a different set of results [21].

To make a numerical assessment of our experimental results, the positron lifetime in GaN was theoretically calculated by using the model of supercell (2 × 1 × 1 unitcells) in an unrelaxed structure. A lifetime of 154.8 ps was obtained by adopting the QMCGGA (quantum Monte Carlo generalized gradient approximation) form of enhancement factor [24,25]. The lifetime component τ_1 (154.6–157.0 ps) in our experimental results, which corresponds to the annihilation lifetime in GaN, is in quantitative agreement with our theoretical calculation (154.8 ps) and previous experimental studies (in the range between 155 and 165 ps) [26–28]. This clearly demonstrated the reliability of our SiPM-PAL measurement system.

The count rate and time resolution (from the analysis of PAL spectrum by using LTv9 program) of SiPM-PAL spectrometer are also listed in Table 2. Thereafter, variation of time resolution of SiPM-PAL spectrometer as a function of scintillator length is plotted in Fig. 8. The results indicate that, with scintillator length decreasing from 20.0 to 5.0 mm, the time resolution is significantly optimized for both two types of scintillators. For LYSO, a improvement of time resolution of 24.7% is achieved with scintillator length decreasing from 20.0 to 5.0 mm. While for LFS-3 scintillator, the time resolution optimizes 22.3% as scintillator length decreases from 20.0 to 5.0 mm. The improvement of time resolution with decreasing scintillator length agrees well with the CRT results in Fig. 5.

The variation of count rate (activity of ^{22}Na source: approximately 1.85 MBq) of SiPM-PAL spectrometer as a function of scintillator length is exhibited in Fig. 9. It is easy to see that, the count rate of SiPM-PAL spectrometer has similar growth tendencies as scintillator length increases from 5.0 to 20.0 mm for LYSO and LFS-3 scintillators. The variations of two scintillators could be divided into two distinct stage. In the first stage (scintillator length increasing from 5.0 to 13.8 mm),

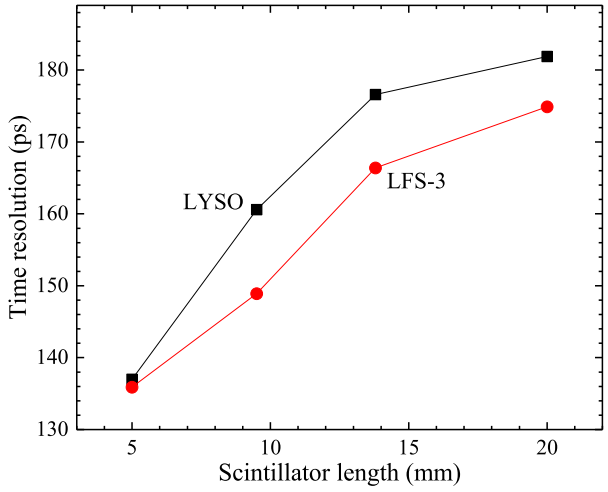

Fig. 8. Time resolution as a function of scintillator length for LYSO and LFS-3.

count rate increases almost three times. In the second stage (scintillator length from 13.8 to 20.0 mm), only a slight increment of count rate (3.6 cps for LYSO, 1.2 cps for LFS-3) could be observed. These results enable us to balance time resolution and count rate of SiPM-PAL spectrometer in the future.

4. Conclusion

In this work, a new SiPM-based PAL spectrometer was successfully developed by using LYSO and LFS-3 scintillators, and a digital oscilloscope. The dependences of SiPM bias voltage, LED threshold,

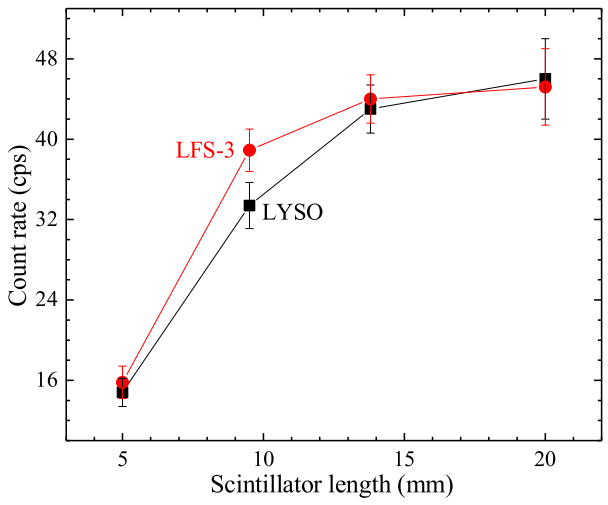

Fig. 9. Count rate as a function of scintillator length for LYSO and LFS-3.

and scintillator length on CRT were studied to determine the best experimental condition of SiPM-PAL spectrometer. PAL measurements were carried out at the optimal SiPM bias voltage and LED threshold. PAL spectra of GaN measured by SiPM-PAL spectrometer with different scintillators (including scintillator material and length) give results in good agreement with previous measurements [26–28] and with theory. High time resolutions of 135.9 and 137.0 ps were achieved for the SiPM-PAL spectrometer by using LFS-3 and LYSO scintillators ($3 \times 3 \times 5$ mm^3), respectively. This demonstrates that SiPM could be utilized to construct PAL spectrometer to achieve high resolution at low cost.

Declaration of competing interest

The authors declare that they have no known competing financial interests or personal relationships that could have appeared to influence the work reported in this paper.

CRediT authorship contribution statement

H.B. Wang: Conceptualization, Methodology, Investigation, Data curation, Software, Validation, Formal analysis, Writing - original draft, Writing - review & editing. **Q.H. Zhao:** Software, Data curation, Formal analysis. **H. Liang:** Writing - reviewing & editing, Resources. **B.C. Gu:** Formal analysis. **J.D. Liu:** Writing - review & editing. **H.J. Zhang:** Writing - review & editing, Supervision. **B.J. Ye:** Writing - review & editing, Resources, Supervision.

Acknowledgments

The authors wish to thank Saint-Gobain and Zecotek Photonics for providing LYSO and LFS-3 scintillators, respectively. We are grateful to R. Ye, X.X. Han, L.H. Cong, and X.J. Ni of USTC for their valuable suggestions and discussions. This work was supported by the National Key R&D Program of China (Grant No. 2019YFA0210000), the National Natural Science Foundation of China (Grant No. 11875248, 11775215, and 11975225), and the Special Fund for Research on National Major Research Instruments, China (Grant No. 11527811).

References

[1] P. Hautojärvi, C. Corbel, Positron spectroscopy of defects in metals and semiconductors, Positron Spectroscopy of Solids, Vol. 125, 1995, pp. 491–532.
[2] M. Biasini, Study of the Fermi surface of molybdenum and chromium via positron annihilation experiments, Physica B 275 (4) (2000) 285–294.
[3] R.S. Brusa, G.P. Karwasz, N. Tiengo, A. Zecca, F. Corni, R. Tonini, G. Ottaviani, Formation of vacancy clusters and cavities in He-implanted silicon studied by slow-positron annihilation spectroscopy, Phys. Rev. B 61 (15) (2000) 10154.
[4] M. Laval, M. Moszyński, R. Allemand, E. Cormoreche, P. Guinet, R. Odru, J. Vacher, Barium fluoride—inorganic scintillator for subnanosecond timing, Nucl. Instrum. Methods Phys. Res. 206 (1–2) (1983) 169–176.
[5] H. Rajainmäki, High-resolution positron lifetime spectrometer with BaF2 scintillators, Appl. Phys. A 42 (3) (1987) 205–208.
[6] J. De Vries, F. Kelling, Fast timing with photomultiplier dynode pulses, Nucl. Instrum. Methods Phys. Res. A 262 (2–3) (1987) 385–393.
[7] J. De Vries, A. Zecca, R. Brusa, R. Grisenti, S. Oss, Fast timing with hamamatsu R2083Q photomultipliers, Nucl. Instrum. Methods Phys. Res. A 275 (1) (1989) 194–196.
[8] F. Bečvář, J. Čížek, L. Lešták, I. Novotnỳ, I. Procházka, F. Šebesta, A high-resolution BaF2 positron-lifetime spectrometer and experience with its long-term exploitation, Nucl. Instrum. Methods Phys. Res. A 443 (2–3) (2000) 557–577.
[9] K. Rytsölä, J. Nissilä, J. Kokkonen, A. Laakso, R. Aavikko, K. Saarinen, Digital measurement of positron lifetime, Appl. Surf. Sci. 194 (1–4) (2002) 260–263.
[10] H. Saito, Y. Nagashima, T. Kurihara, T. Hyodo, A new positron lifetime spectrometer using a fast digital oscilloscope and BaF2 scintillators, Nucl. Instrum. Methods Phys. Res. A 487 (3) (2002) 612–617.
[11] J. Nissilä, K. Rytsölä, R. Aavikko, A. Laakso, K. Saarinen, P. Hautojärvi, Performance analysis of a digital positron lifetime spectrometer, Nucl. Instrum. Methods Phys. Res. A 538 (1–3) (2005) 778–789.
[12] S. España, L. Fraile, J. Herraiz, J.M. Udías, M. Desco, J. Vaquero, Performance evaluation of SiPM photodetectors for PET imaging in the presence of magnetic fields, Nucl. Instrum. Methods Phys. Res. A 613 (2) (2010) 308–316.
[13] G. Collazuol, G. Ambrosi, M. Boscardin, F. Corsi, G.F. Dalla Betta, A. Del Guerra, N. Dinu, M. Galimberti, D. Giulietti, L.A. Gizzi, et al., Single photon timing resolution and detection efficiency of the IRST silicon photo-multipliers, Nucl. Instrum. Methods Phys. Res. A 581 (1–2) (2007) 461–464.
[14] A. Ronzhin, M. Albrow, K. Byrum, M. Demarteau, S. Los, E. May, E. Ramberg, J. Va'vra, A. Zatserklyaniy, Tests of timing properties of silicon photomultipliers, Nucl. Instrum. Methods Phys. Res. A 616 (1) (2010) 38–44.
[15] S. Gundacker, E. Auffray, N. Di Vara, B. Frisch, H. Hillemanns, P. Jarron, B. Lang, T. Meyer, S. Mosquera-Vazquez, E. Vauthey, et al., SiPM time resolution: From single photon to saturation, Nucl. Instrum. Methods Phys. Res. A 718 (2013) 569–572.
[16] S. Seifert, R. Vinke, H.T. van Dam, H. Löhner, P. Dendooven, F.J. Beekman, D.R. Schaart, Ultra precise timing with SiPM-based TOF PET scintillation detectors, in: Nuclear Science Symposium Conference Record (NSS/MIC), 2009 IEEE, IEEE, 2009, pp. 2329–2333.
[17] K. Doroud, A. Rodriguez, M. Williams, A. Zichichi, R. Zuyeuski, Comparative timing measurements of LYSO and LFS to achieve the best time resolution for TOF-PET, in: 2014 IEEE Nuclear Science Symposium and Medical Imaging Conference (NSS/MIC), IEEE, 2014, pp. 1–4.
[18] C. Bircher, Y. Shao, Investigation of crystal surface finish and geometry on single LYSO scintillator detector performance for depth-of-interaction measurement with silicon photomultipliers, Nucl. Instrum. Methods Phys. Res. A 693 (2012) 236–243.
[19] H. Kim, W.-S. Choong, N. Eclov, F. Abu-Nimeh, C.-T. Chen, C.-M. Kao, A performance comparison of LFS and LYSO scintillators for TOF PET, in: 2015 IEEE Nuclear Science Symposium and Medical Imaging Conference (NSS/MIC), IEEE, 2015, pp. 1–2.
[20] S. Gundacker, A. Knapitsch, E. Auffray, P. Jarron, T. Meyer, P. Lecoq, Time resolution deterioration with increasing crystal length in a TOF-PET system, Nucl. Instrum. Methods Phys. Res. A 737 (2014) 92–100.
[21] J. Kansy, Microcomputer program for analysis of positron annihilation lifetime spectra, Nucl. Instrum. Methods Phys. Res. A 374 (2) (1996) 235–244.
[22] J.V. Olsen, P. Kirkegaard, N.J. Pedersen, M. Eldrup, PALSfit: A new program for the evaluation of positron lifetime spectra, Phys. Status Solidi (c) 4 (10) (2007) 4004–4006.
[23] P. Kirkegaard, J.V. Olsen, M. Eldrup, N.J. Pedersen, PALSfit: A computer program for analysing positron lifetime spectra, in: Risø National Laboratory for Sustainable Energy, Technical University of Denmark, Roskilde, Denmark, Risø-R-1652, Citeseer, 2009.
[24] M.J. Puska, R.M. Nieminen, Theory of positrons in solids and on solid surfaces, Rev. Modern Phys. 66 (3) (1994) 841.
[25] W. Zhang, B. Gu, J. Liu, B. Ye, Accurate theoretical prediction on positron lifetime of bulk materials, Comput. Mater. Sci. 105 (2015) 32–38.
[26] K. Saarinen, T. Laine, S. Kuisma, J. Nissilä, P. Hautojärvi, L. Dobrzynski, J. Baranowski, K. Pakula, R. Stepniewski, M. Wojdak, et al., Observation of native Ga vacancies in GaN by positron annihilation, MRS Online Proc. Library Arch. 482 (1997).
[27] K. Saarinen, J. Nissilä, P. Hautojärvi, J. Likonen, T. Suski, I. Grzegory, B. Lucznik, S. Porowski, The influence of Mg doping on the formation of Ga vacancies and negative ions in GaN bulk crystals, Appl. Phys. Lett. 75 (16) (1999) 2441–2443.
[28] S. Hautakangas, I. Makkonen, V. Ranki, M. Puska, K. Saarinen, X. Xu, D.C. Look, Direct evidence of impurity decoration of Ga vacancies in GaN from positron annihilation spectroscopy, Phys. Rev. B 73 (19) (2006) 193301.